

Original Research Article

Estimation of Surface and Subsurface Soil Moisture using Microwave Remote Sensing

ABSTRACT

Accurate measurement and monitoring of surface and subsurface soil moisture is essential for understanding hydrological processes, crop growth modeling, crop water requirement, and climate studies. It's important to note that estimating of surface and subsurface soil moisture using remote sensing is a complex process that requires careful calibration, validation, and consideration of factors such as vegetation cover, soil type, and surface roughness. Accurate measurement of the soil moisture content in the root zone is essential for precise irrigation authority and plant water stress evaluation. However, the two existing passive microwave satellite missions, Soil Moisture and Ocean Salinity (SMOS) and Soil Moisture Active Passive (SMAP), that operate at L-band, can only estimate the top 5 cm of soil moisture. Microwave remote sensing has proven to be a valuable tool for non-invasive soil moisture estimation. This research aims to investigate and develop a methodology for estimating surface and subsurface soil moisture using microwave data from Sentinel-1. The study was conducted to establish the relationship between surface & subsurface soil moisture and the backscatter coefficient derived using the Sentinel-1 SAR microwave remote sensing satellite imagery, in the Godhra region. Two seasons namely summer (zaid) and monsoon (Kharif) were taken into consideration to build up the relationship between surface soil moisture and co-polarization backscatter coefficient (σ_{VV}). For the summer (zaid) and monsoon (Kharif) seasons, the co-polarization backscatter coefficient (σ_{VV}) and surface soil moisture were found to have a correlation in terms of R^2 as 0.91 and 0.90, respectively. The study explores the relationship between microwave signals and surface soil moisture content (0-5 cm) and then the relationship between surface soil moisture and soil moisture at various depths were also modeled thereby contributing to improved soil moisture estimation techniques and applications. The value of the coefficient of determination (R^2) of surface soil moisture to soil moisture at 20 cm, 40 cm, and 60 cm depths were found to be 0.60, 0.51, and 0.46, respectively, in the summer (zaid) season. The value of the coefficient of determination (R^2) of surface soil moisture to soil moisture at 20 cm, 40 cm, 60 cm, 80 cm, and 100 cm

depths were found to be 0.83, 0.61, 0.51, 0.26, and 0.13, respectively. According to the study, it is observed that the relationship between co-polarization backscatter coefficient (σ_{VV}) and soil moisture weakens as the depth of soil moisture increases. Overall, the regression models developed between the co-polarization backscatter coefficient (σ_{VV}) and surface soil moisture showed very good results, whereas the regression models developed between the surface soil moisture and soil moisture at various depths showed reasonably acceptable results up to the depth of 60 cm. The findings in the present study suggest that Sentinel-1A C-band SAR data can be used to estimate surface as well as it can be extended getting satisfactory results upto the depth of 60 cm, in terms of associated surface and subsurface soil moisture modeling using regression equations.

Keywords: Surface and Subsurface soil moisture, Sentinel-1, Synthetic Aperture Radar (SAR), Microwave, Monsoon and Summer seasons, Godhra

1. INTRODUCTION

There is a crucial need for the development of economically viable agricultural practices as the global population continues to increase and water supplies become scarcer because of climate change, demand from other beneficial uses, and more regulation of agriculture use (Boretti and Rosa, 2019). To better understand the connections between climate dynamics, hydrology, agriculture, drought, and food security, soil moisture plays a crucial and important variable (Gao et al., 2014; Sadri et al., 2020; Ram et al., 2023). In order to maximize crop yield, farmers must have information on soil moisture. Long-term soil moisture data combined with climate data can provide an understanding of patterns, agricultural thresholds, and losses (Lin et al., 2018).

The subsurface soil moisture also known as Root Zone Soil Moisture (RZSM), or profile soil moisture is regarded as one of the most crucial factors influencing the growth of vegetation. Therefore, precise regional estimates of subsurface soil moisture are useful for a variety of applications, including the assessment of root zone soil moisture using remote sensing and vadose zone modelling (Shukla and Mintz, 1982; Hanson and Peters, 1999; Pauwels et al., 2001; Yu et al., 2014; Balas and Thakor, 2021).

Surface soil moisture (SSM) generally indicates the soil moisture content of soils upto the depth of 5 cm. The majority of remote sensing technologies are limited to determining SSM. Sub-surface soil moisture is the soil moisture content of soils at deeper levels where plant root intake of water occurs and is significantly more relevant to decision-

Comment [h1]: Consider reframing the sentence to convey the exact meaning! Also, the sentence is too long, needs to be shortened!

Comment [h2]: Source?

Comment [h3]: Spacing error

making and management (Bauer-Marschallinger et al., 2018). A precise estimation of subsurface soil moisture is necessary to evaluate the plant water availability and for the scheduling of irrigation. Soil moisture monitoring approaches are rapidly expanding and evolving because of the launch of recently developed satellites, other sensing technologies, and more effective modeling capabilities (Peddinti et al., 2018). Over the past few years, several models (theoretical and empirical) have been developed for obtaining surface soil moisture at a depth of 0-5 cm using either active or passive microwave technology and establishing the correlation between the soil dielectric coefficient and water content (Petropoulos et al., 2015).

The SSM data, which can be acquired either through satellites, can typically be used to extrapolate the subsurface soil moisture (Sabater et al., 2007). The setup of many sensors in the subsurface network can be expensive and time-consuming, and it is likely to have an impact on the soil properties. This makes spatially distributed sub-surface soil moisture challenging (González-Teruel et al., 2019). Richard's equation-based complex process models for predicting soil moisture dynamics on a wide scale can be computationally expensive due to the vast amount of data needed for parameterization. Surface and subsurface soil moisture estimations are currently utilizing data-driven forecast technologies including artificial neural networks (ANN), Random Forest (RF), and statistical learning tools like Support Vector Machines (SVM) (Yu et al., 2012; Hassan-Esfahani et al., 2015; Carranza et al., 2021). In the preceding few years, Machine Learning (ML) techniques have become widespread in soil hydrology research, and they are now more frequently used to estimate model-derived subsurface soil moisture by ANN (Carranza et al., 2021).

Microwave remote sensing is the most promising method for precisely monitoring soil moisture over a wide area because microwaves can penetrate the land surface to a certain depth and capture changes in soil dielectric characteristics caused by changes in the amount of water in the soil. Different indices and algorithms have been made for calculating subsurface soil moisture by linking SSM time series data (Wagner et al., 1999). Several microwave remote-sensing soil moisture technologies have been extensively used in scientific research and applications and are confirmed to have a significant correlation with ground-measured data (Owe et al., 2001; Dorigo et al., 2017). Meanwhile, the microwave sensors mounted on the satellites are only able to reach a depth of a few centimeters into the soil's surface and can't acquire data on soil moisture at greater depths (Baldwin et al., 2019). However, there still remains a need to measure subsurface soil moisture in the top meter of

Comment [h4]: Source?

soil because this information is critical for modeling and forecasting processes like the onset of drought, plant growth, and chemical transfer through the soil (Denmead et al., 1962; Malone et al., 2004; Narasimhan et al., 2005).

This study was conducted to investigate and develop a methodology for simulating surface and subsurface soil moisture using microwave remote sensing data. The availability of accurate and timely information on soil moisture is crucial for various applications, such as agriculture, hydrology, and climate studies. Microwave remote sensing offers the capability to penetrate through the soil and retrieve information about the moisture content at different depths. This research focuses on the utilization of microwave data to estimate surface and possible direct application to estimate subsurface soil moisture and explores to develop a relationship between the measured microwave signals and the underlying soil moisture profiles. The following is an outline of the paper's structure: The study area, method, and data are described in Section 2; the results are illustrated in Section 3; and the discussion and findings are presented in Section 4.

Comment [h5]: Remove this!

2. MATERIALS AND METHODS

2.1 Study Area Location

The study area falls in the Panchmahal district of Gujarat, India as seen in Fig. 1, and was selected for the current research work. The research area is approximated as 772 km² in size, has an estimated population of 4,62,516 (census-2011), and is bounded by latitudes 22°41'51" N to 22°53'35" N and longitudes 73°21'08" E to 73°51'11" E. Godhra sub-district is located in the Middle Gujarat Agro Climatic Zone-III, which is semi-arid and has an average annual rainfall vary between 650 to 750 mm. The study area's soil type is sandy loam, and its lowest and highest temperatures range from 6 °C (cold winter) to 44 °C (hot summer).

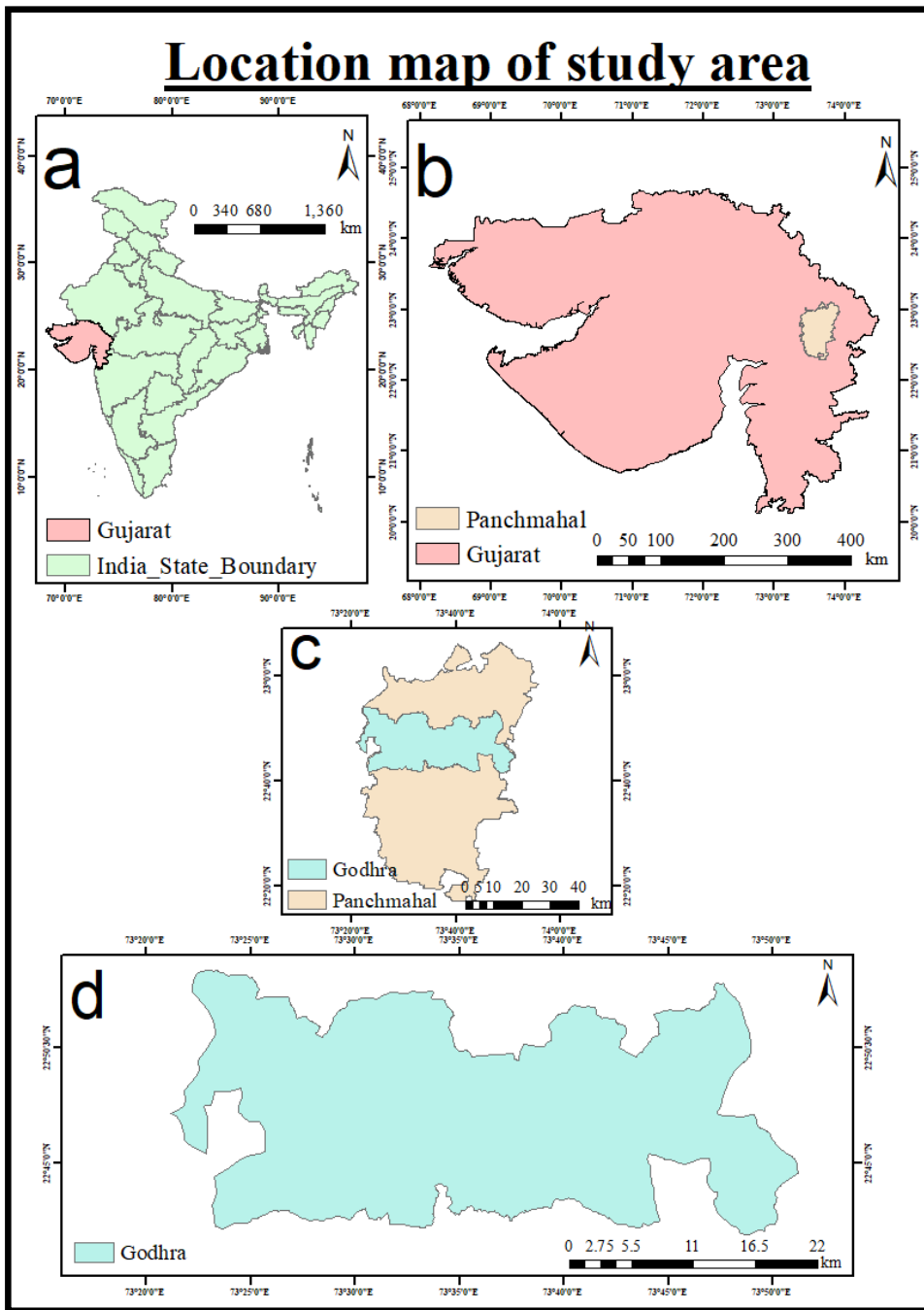


Fig. 1: Study area location (a) Indian administrative boundary (b) Gujarat state administrative boundary (c) Panchmahal district administrative boundary (d) Godhra tehsil administrative boundary

2.2 Data Collection and Analysis

The soil moisture was measured at an interval of 20 cm stepped i.e., surface, 20 cm, 40 cm, 60cm, 80 cm, and 100 cm considering the timing of overpassing of Sentinel-1 from March-2021 to November-2021. Throughout the study period, there were eight different locations (4 for each season) and two different seasons, namely summer (zaid) and monsoon (Kharif) were selected to measure the soil moisture for different depths. Out of eight locations, four were assigned to each season, and these four locations were also distributed randomly in four quarter divisions, over the full study region as shown in Fig. 2. Depth wise total of six soil samples were taken from each point (surface, 20, 40, 60,80 and 100 cm).

We determined soil moisture content up to 60 cm and 100 cm depth during the summer (zaid) season and monsoon season (kharif), respectively with the help of a hand-held auger hoe and knife. Soil samples were collected at an interval of 20 cm depth by digging a hole and packed in an airtight bag. A total of 40 samples were collected in both seasons: 24 (6×4) during the monsoon season (Kharif) and 16 (4×6) during the summer (zaid) season.

Comment [h6]: This interval, is it vertical or horizontal and what is the criteria for the 20 cm, 40 cm

Comment [h7]: The specific coordinates of the locations should be mentioned!

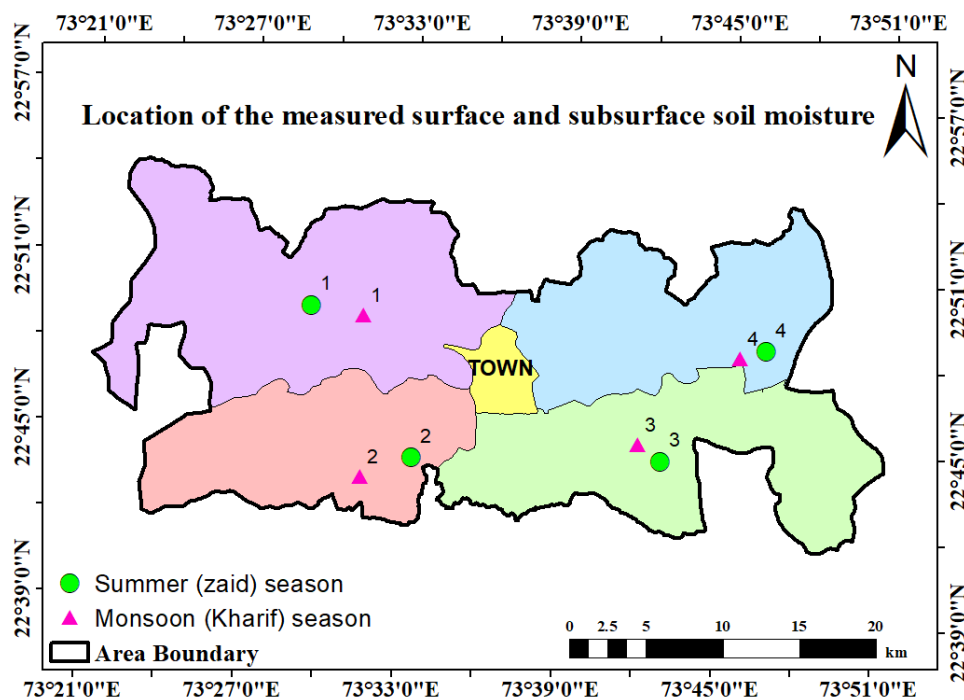


Fig. 2: Representation of geolocated surface and subsurface soil moisture data collected in both seasons

Many alternative techniques have been available in recent years to measure soil moisture content. Direct and indirect methods are generally used to determine soil moisture. Direct methods measure the soil moisture based on a calculation of the difference between the before and after drying of the soil. In indirect approaches, the moisture content of the soil is measured using sensors and other characteristics that have an impact on it, depending on the device's accuracy. Therefore, compared to indirect methods such as the dielectric technique, tensiometry method, etc., the gravimetric approach (direct method) is more reliable and provides accurate soil moisture. A gravimetric soil moisture determination method was used in this study (Shih and Jordan, 1992).

The soil samples were tightly packed in airtight polythene bags. A weighing balance was used to determine the wet and dry weight of the soil samples as shown in Fig. 3. Each sample was then placed in a hot air oven dryer at 105° C for 24 hours to determine the dry weight (Aniley et. al., 2018). The gravimetric moisture content (MC) estimation method was used to determine the soil moisture (Eq.-1).

$$MC, \% = \frac{\text{Wet weight} - \text{Dry weight}}{\text{Dry weight}}$$

1





Fig. 3: Collection and oven drying of soil samples

2.3 Satellite Data

The Sentinel-1 mission consists of a pair of two polar-orbiting satellites that operate during the day and night along with C-band ($\lambda = 5.6$ cm) Synthetic Aperture Radar (SAR) imaging to collect data in all weather conditions. Sentinel-1 designed by the European Space Agency (ESA) having spatial and temporal resolutions are 10 m and 6-day, respectively was used in this study. It has four different acquisition modes: Strip Map (SM), Interferometric Wide swath (IW), Extra Wide swath (EW), and Wave (WV) modes. As stated in Table 1, Sentinel-1 SAR data for various dates used in the study were retrieved from <https://scihub.copernicus.eu>.

Table 1: Sentinel-1 over passing dates

Sl. No.	Date	Sl. No.	Date
Summer season		Monsoon season	
1	05-03-2021	5	27-07-2021
2	10-04-2021	6	20-08-2021
3	16-05-2021	7	13-09-2021
4	09-06-2021	8	07-10-2021

2.4 Software used

ArcGIS (v-10.3) and SNAP (v-8.0.0) were used in this study to estimate the soil moisture using Remote Sensing and GIS. Sentinel Applications Platform (SNAP) released by European Space Agency (ESA) in 2014 was downloaded from <https://step.esa.int/main/download/snap-download/>.

2.5 Workflow to Pre-process the Sentinel-1 GRD Product to extract the co-polarization (σ_{VV}) and cross-polarization (σ_{VH})

This workflow is applicable within the Sentinel Application Platform (SNAP). The pre-processing workflow is a series of nine processing steps that are designed to eliminate error propagation in following operations as much as possible (Filipponi, 2019). All the steps are illustrated in the flowchart as shown in Fig. 4 and described simultaneously.

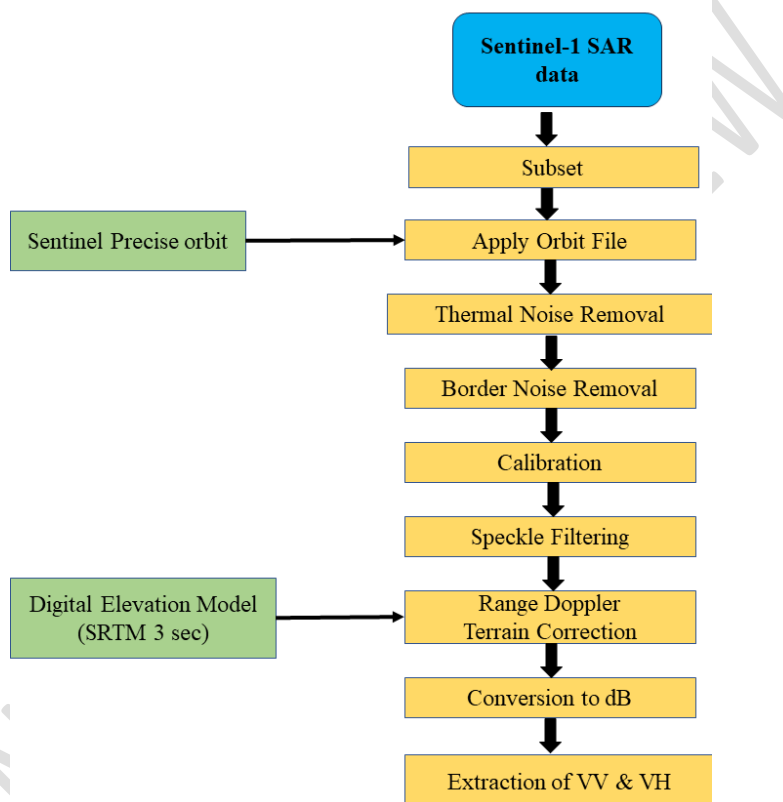


Fig. 4: Methodology flowchart of data analysis

The SNAP procedure of applying a precise orbit enables the automated download and update of orbit state vectors for each SAR scene in its product metadata, providing precise satellite location and velocity information. Thermal noise must be corrected or removed to normalize the backscatter signal throughout the full SAR image, which is necessary for both qualitative and quantitative SAR data application. Sentinel-1 images are affected by the so-called border noise effect. These noises, or non-zero artifacts, appear as a narrow strip along the range and azimuth directions' boundaries. Such noise must be eliminated before further processing. Calibration is the process of converting digitized pixel values to radiometrically

calibrated SAR backscatter. Speckle filtering is a technique for improving image quality by diminishing speckles. A digital elevation model is used as an input, and range doppler terrain correction shifts all pixels to their proper positions. The final step is to convert the unitless backscatter coefficient (σ_0) into dB using a logarithmic transformation. At the end, co-polarization (σ_{VV}) and cross-polarization (σ_{VH}) were extracted using latitude and longitude locations.

2.6 Linear Regression

Linear regression attempts to model the relationship between two variables by fitting a linear equation to observed data. One variable is an explanatory variable, and the other is considered to be a dependent variable. The least-squares approach is the most often used method for fitting a regression line. The best-fitting line for the observed data is determined by minimizing the sum of the squares of the vertical deviations from each data point to the line. It is given by the following equation-2.

$$Y = \beta_0 + \beta_1 X_1$$

Where,

Y	=	Dependent or predicted variable
β_1	=	Regression coefficient
X_1	=	Independent or predictor variable
β_0	=	Intercept

Comment [h8]: (2)

2

Comment [h9]: (2)

3 RESULTS

3.1 Variability of Soil Moisture

In summer (zaid) and monsoon (Kharif) seasons surface soil moisture varies from 0.93 % to 2.21 % and 10.25 % to 19.23 %, respectively. Whereas, in summer (zaid) and monsoon (Kharif) seasons, subsurface soil moisture varies from 0.82 % to 2.37 % and 9.85 % to 20.72 %, respectively for the study area. Variability of subsurface soil moisture at particular depths (surface/20/40/60/80/100 cm) for different locations (1, 2, 3, and 4) and at particular locations (1/2/3/4) for different depths (surface, 20, 40, 60,80 and 100 cm) for both seasons are depicted in Figs. 5 to 8. The variability of subsurface soil moisture in both seasons is significantly distinguished. In the summer (zaid) season, the soil moisture is low compared to monsoon (zaid) season. The variability of subsurface soil moisture in every four locations also differed from each other and at particular location depth wise it also varies

marginally in the summer (zaid) season. In the case of the monsoon (zaid) season, the subsurface soil moisture variability was found significantly higher compared to the summer (zaid) season. as shown in Figs. 5 to 8.

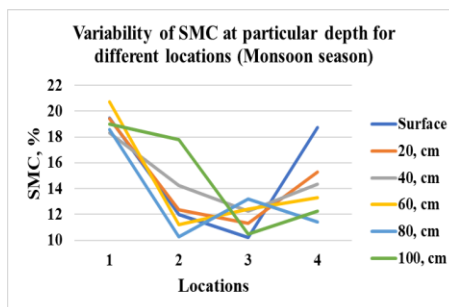
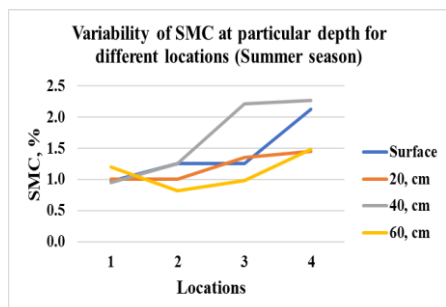


Fig. 5: Location-wise soil moisture variation in the summer (zaid) season

Fig. 6: Location-wise soil moisture variation in the monsoon (kharif) season

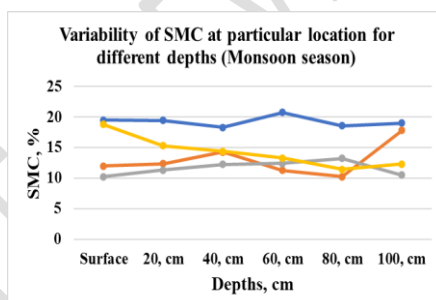
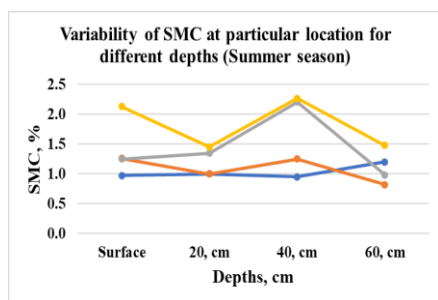


Fig. 7: Depth-wise soil moisture variation in the summer (zaid) season

Fig. 8: Depth-wise soil moisture variation in the monsoon (kharif) season

3.2 Modelling of Backscatter Co-polarization (σ_{VV}) with Surface Soil Moisture

Due to problematic conditions and drudgery in subsurface soil sampling, we were not gathered data in bulk. Keeping this in view we established a relationship of surface soil moisture with co-polarization (σ_{VV}) because among both polarizations (σ_{VV} and σ_{VH}), the strong relation to soil moisture was found with co-polarization (σ_{VV}) only. In the further analysis, we used only co-polarization (σ_{VV}) for the subsurface soil moisture. The relationship of co-polarization (σ_{VV}) with surface soil moisture is shown in Fig. 9 and 10 with R^2 values are 0.91 and 0.90 for summer (zaid) and monsoon (Kharif) seasons, respectively suggesting a strong correlation. A little bit higher correlation (+ 0.1) was found in the summer (zaid) season compared to the monsoon season (Kharif).

Comment [h10]: Reframe this sentence to convey the idea properly

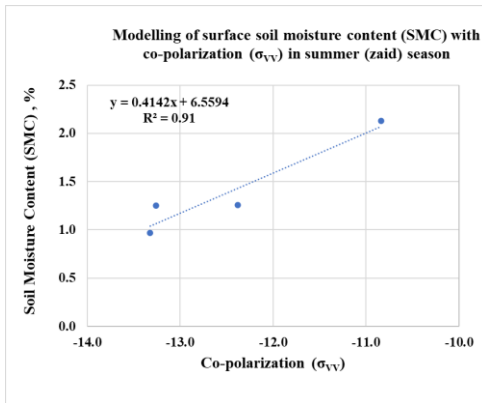


Fig. 9: Correlation between surface soil moisture and co-polarization (σ_{VV}) in summer (zaid) season

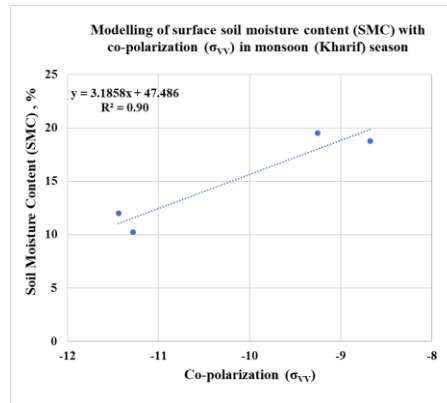


Fig. 10: Correlation between surface soil moisture and co-polarization (σ_{VV}) in monsoon (Kharif) season

3.3 Modelling of Surface Soil Moisture to Subsurface Soil Moisture

To measure the subsurface soil moisture at different depths i.e., 20 cm, 40 cm, 60 cm, 80 cm, and 100 cm we established linear regression with surface soil moisture for both seasons. In the summer (zaid) season subsurface soil moisture was measured up to 60 cm depth at an interval of 20 cm so, we obtained three relationships while in the monsoon (kharif) season, we reached up to 100 cm depth so, five relationships were obtained.

In the summer (zaid) season, the value of the coefficient of determination (R^2) of surface soil moisture with 20 cm, 40 cm, and 60 cm are 0.60, 0.51, and 0.46, respectively (Fig. 11) whereas in monsoon (Kharif) season the value of the coefficient of determination (R^2) of surface SMC with 20 cm, 40 cm, 60 cm, 80 cm, and 100 cm is 0.83, 0.61, 0.51, 0.26 and 0.13, respectively (Fig. 12) was found. The result indicates that increase in depth from the surface to the subsurface, the relation of surface SMC with stepped depth becomes weak. Similar results were also obtained in the monsoon (kharif) season. In the monsoon (kharif) season, strong relation was observed compared to the summer (zaid) season for the first three depths i.e., 20 cm, 40 cm and 60 cm as shown in Fig. 12. There is not much of a correlation when looking more deeply below 60 cm in the monsoon (kharif) season.

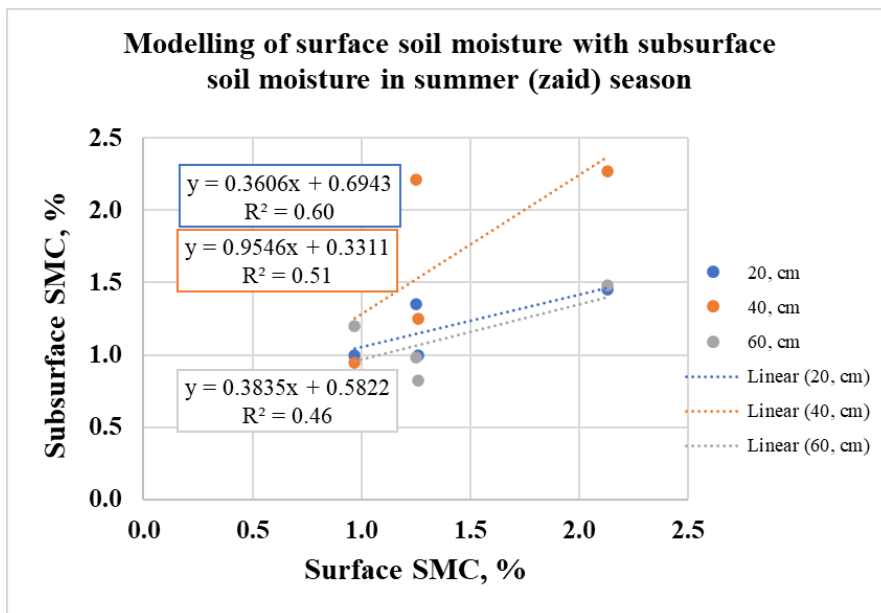


Fig. 11: Relationship between surface and subsurface soil moisture in summer (zaid) season

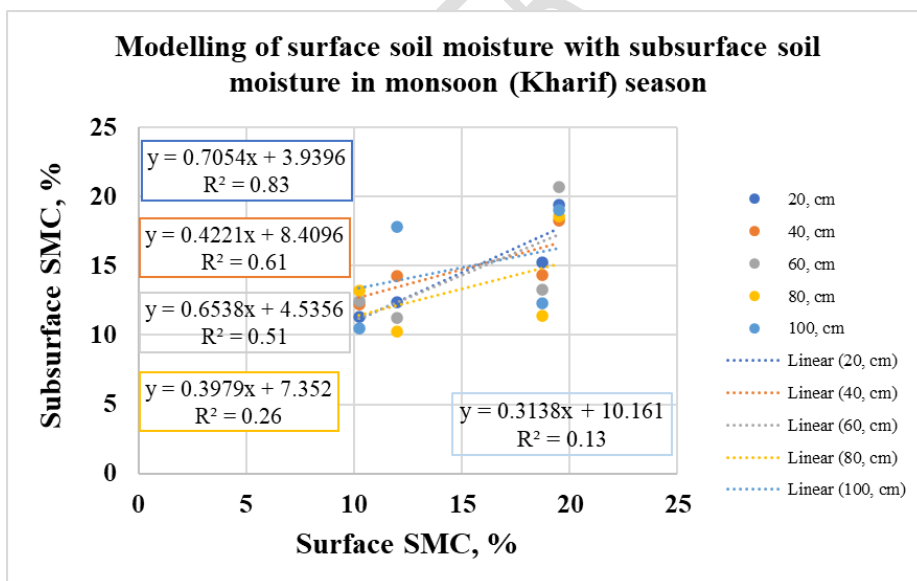


Fig. 12: Relationship between surface and subsurface soil moisture in monsoon (kharif) season

4 CONCLUSIONS

The study was conducted to simulate the surface soil moisture and to estimate the subsurface soil moisture based on remotely sensed microwave C-band Synthetic Aperture Radar (SAR) data of Sentinel-1 satellite in Godhra, Panchmahl, Gujarat. A total of 40 soil samples were collected from different locations in the Godhra taluk in accordance with the Sentinel-1 passage date. The gravimetric approach was used to determine the in-situ soil moisture content. Sentinel Application Platform (SNAP) software's open-source tool was used to analyze the Sentinel-1 SAR microwave data and to extract the backscattering coefficient. Soil moisture as measured in the field (MC, %) was used as the dependent variable, whereas co-polarization (σ_{VV}) was used as the independent variable. The association between the backscatter coefficient co-polarization (σ_{VV}) and the surface soil moisture and then its relationship with subsurface soil moisture was established using the linear regression model. Co-polarization (σ_{VV}) and surface soil moisture were found to be associated with R^2 values of 0.91 and 0.90 for the summer (zaid) and monsoon (Kharif), respectively. Furthermore, considering the subsurface soil moisture, the study showed that as depth increased, the relationship between co-polarization (σ_{VV}) and soil moisture decreased. According to the study's findings, Sentinel-1A C-band SAR data can be used to measure surface as well as the subsurface soil moisture at the regional level.

Comment [h11]: contents

REFERENCES

- Aniley, A. A., Kumar, N., & Kumar, A. (2018). Soil moisture sensors in agriculture and the possible application of nanomaterials in soil moisture sensors fabrication. *International Journal of Advanced Engineering Research and Technology*, 6(1), 2348-8190.
- Balas, D., & Thakor, D. (2021). Development of rainfall simulator to observe the real field runoff on sweet orange (*Citrus X sinensis*) orchard. *The Pharma Innovation Journal*, 10(11): 1312-1317
- Baldwin, D., Manfreda, S., Lin, H., & Smithwick, E. A. (2019). Estimating root zone soil moisture across the Eastern United States with passive microwave satellite data and a simple hydrologic model. *Remote Sensing*, 11(17), 2013.
- Bauer-Marschallinger, B., Freeman, V., Cao, S., Paulik, C., Schaufler, S., Stachl, T., Modanesi, S., Massari, C., Ciabatta, L., Brocca, L. & Wagner, W. (2018). Toward global soil

moisture monitoring with Sentinel-1: Harnessing assets and overcoming obstacles. *Transactions on Geoscience and Remote Sensing*, 57(1), 520-539.

Boretti, A., & Rosa, L. (2019). Reassessing the projections of the world water development report. *Clean Water*, 2(1), 15.

Carranza, C., Nolet, C., Pezij, M., & van der Ploeg, M. (2021). Root zone soil moisture estimation with Random Forest. *Journal of Hydrology*, 593, 125840.

Denmead, O. T., & Shaw, R. H. (1962). Availability of soil water to plants as affected by soil moisture content and meteorological conditions 1. *Agronomy Journal*, 54(5), 385-390.

Dorigo, W., Wagner, W., Albergel, C., Albrecht, F., Balsamo, G., Brocca, L., Chung, D., Ertl, M., Forkel, M., Gruber, A. & Haas, E., (2017). ESA CCI Soil Moisture for improved Earth system understanding: State-of-the art and future directions. *Remote Sensing of Environment*, 203, 185-215.

Gao, X., Wu, P., Zhao, X., Wang, J., & Shi, Y. (2014). Effects of land use on soil moisture variations in a semi-arid catchment: implications for land and agricultural water management. *Land Degradation & Development*, 25(2), 163-172.

González-Teruel, J. D., Torres-Sánchez, R., Blaya-Ros, P. J., Toledo-Moreo, A. B., Jiménez-Buendía, M., & Soto-Valles, F. (2019). Design and calibration of a low-cost SDI-12 soil moisture sensor. *Sensors*, 19(3), 491.

Hanson, B. R., & Peters, D. W. (1999). Using dielectric soil moisture sensors for irrigation scheduling. *Irrigation of Horticultural Crops*, 537 (471-477).

Hassan-Esfahani, L., Torres-Rua, A., Jensen, A., & McKee, M. (2015). Assessment of surface soil moisture using high-resolution multi-spectral imagery and artificial neural networks. *Remote Sensing*, 7(3), 2627-2646.

Lin, B. B., Egerer, M. H., Liere, H., Jha, S., & Philpott, S. M. (2018). Soil management is key to maintaining soil moisture in urban gardens facing changing climatic conditions. *Scientific Reports*, 8(1), 17565.

Malone, R. W., Ahuja, L. R., Ma, L., Don Wauchope, R., Ma, Q., & Rojas, K. W. (2004). Application of the Root Zone Water Quality Model (RZWQM) to pesticide fate and transport: an overview. *Pest Management Science*, 60(3), 205-221.

Narasimhan, B., & Srinivasan, R. (2005). Development and evaluation of Soil Moisture Deficit Index (SMDI) and Evapotranspiration Deficit Index (ETDI) for agricultural drought monitoring. *Agricultural and Forest Meteorology*, 133(1-4), 69-88.

Owe, M., de Jeu, R., & Walker, J. (2001). A methodology for surface soil moisture and vegetation optical depth retrieval using the microwave polarization difference index. *Transactions on Geoscience and Remote Sensing*, 39(8), 1643-1654.

Pauwels, V. R., Hoeben, R., Verhoest, N. E., & De Troch, F. P. (2001). The importance of the spatial patterns of remotely sensed soil moisture in the improvement of discharge predictions for small-scale basins through data assimilation. *Journal of Hydrology*, 251(1-2), 88-102.

Peddinti, S. R., Kambhammettu, B. V. N. P., Ranjan, S., Suradhaniwar, S., Badnakhe, M. R., Adinarayana, J., & Gade, R. M. (2018). Modeling Soil–Water–Disease Interactions of Flood-Irrigated Mandarin Orange Trees: Role of Root Distribution Parameters. *Vadose Zone Journal*, 17(1), 1-13.

Petropoulos, G. P., Ireland, G., & Barrett, B. (2015). Surface soil moisture retrievals from remote sensing: Current status, products & future trends. *Physics and Chemistry of the Earth*, Parts A/B/C, 83, 36-56.

Ram, B., Gaur, M. L., Patel, G., Kunapara, A., Pampaniya, N., Damor, P., & Balas, D. (2023). Assessment of Diurnal Variability and Region-Specific Connection across Intensity, Depth & Duration of Rainfall. *International Journal of Environment and Climate Change*, 13(9), 595-606.

Sabater, J. M., Jarlan, L., Calvet, J. C., Bouyssel, F., & De Rosnay, P. (2007). From near-surface to root-zone soil moisture using different assimilation techniques. *Journal of Hydrometeorology*, 8(2), 194-206.

Sadri, S., Pan, M., Wada, Y., Vergopalan, N., Sheffield, J., Famiglietti, J.S., Kerr, Y. & Wood, E. (2020). A global near-real-time soil moisture index monitor for food security using integrated SMOS and SMAP. *Remote Sensing of Environment*, 246, 111864.

Shih, S. F., & Jordan, J. D. (1992). Landsat mid-infrared data and GIS in regional surface soil-moisture assessment. *Journal of the American Water Resources Association*, 28(4), 713-719.

Shukla, J., & Mintz, Y. (1982). Influence of land-surface evapotranspiration on the earth's climate. *Science*, 215(4539), 1498-1501.

Wagner, W., Lemoine, G., & Rott, H. (1999). A method for estimating soil moisture from ERS scatterometer and soil data. *Remote Sensing of Environment*, 70(2), 191-207.

Yu, X., Duffy, C., Baldwin, D. C., & Lin, H. (2014). The role of macropores and multi-resolution soil survey datasets for distributed surface–subsurface flow modeling. *Journal of Hydrology*, 516, 97-106.

Yu, Z., Liu, D., Lü, H., Fu, X., Xiang, L., & Zhu, Y. (2012). A multi-layer soil moisture data assimilation using support vector machines and ensemble particle filter. *Journal of Hydrology*, 475, 53-64.

UNDER PEER REVIEW